DEVELOPMENT OF A PHASE SHIFTING REGULATOR FOR POWER FLOW CONTROL IN LOW VOLTAGE GRIDS

Stefan LANG
TU Kaiserslautern – Germany
lang@eit.uni-kl.de

Wolfram H. WELLSSOW
TU Kaiserslautern – Germany
wellssow@eit.uni-kl.de

ABSTRACT

The increasing number of renewable generators, in particular photovoltaic systems in the low voltage networks of rural areas, causes a strong increase of the power flows. As of today, in meshed grids the power flow is not controlled and the thermal limits of cables can be reached or exceeded. As a consequence failures may occur. With the help of phase shifting regulators for low-voltage distribution grids the power flow in a meshed grid can be controlled and thermal overstress can be prevented to a certain extent. A new type of equipment is proposed which can regulate the power flow by applying a control voltage at a certain angle. In this paper, the methods for calculating the control voltage and a design concept for the regulator are presented.

INTRODUCTION

The increase of renewable generators, such as photovoltaic (PV) systems in particular in rural areas, causes high loadings of low-voltage (LV) network feeders. An increase of the voltage magnitudes beyond permissible values can be the consequence [1]. In classical radial distribution grids, besides network expansion, the network operator has various cost-effective options such as reactive power management, voltage-regulated distribution transformers or series regulators. However, these measures do not prevent possible thermal overloading of network elements. In meshed grids the power flow is not controlled and the thermal limits of cables can be reached or exceeded [2]. Currents and power flows distribute according to the given grid impedances and cannot be managed. Aforementioned measures do not apply. However, by using a special phase shifting regulator (PSR) for LV networks the power flow can be controlled. By the integration of such smart devices into the grid the costly expansion of these networks is either preventable or can be delayed.
By applying a control voltage (CV) at a pre-calculated angle, the power flow in a mesh can be controlled [3]. The optimal control angle depends on the network impedance and the phase shift angle of the current with respect to the nodal voltage in the regulated line section.

DETERMINATION OF CONTROL VOLTAGE

Real LV grids are characterized by a high number of loads and generators. However, only a restricted number of measurement points are feasible for cost reasons. Therefore, unknown values have to be estimated by the controller in order to determine the optimum CV. The network in Fig. 1 is used to explain the principle.

Depending on the shown topology, (1) can be derived which provides a general approach for the calculation of $\underline{U}_{CV}$ for networks with a comparable structure but any number of loads and line segments. (2) represents the unknown load currents which are summarized with the impedances to $\underline{U}_{LC}$. Note that this holds true regardless of whether the currents $\underline{I}_{Li}$ are representing loads or in-feeds. [4]

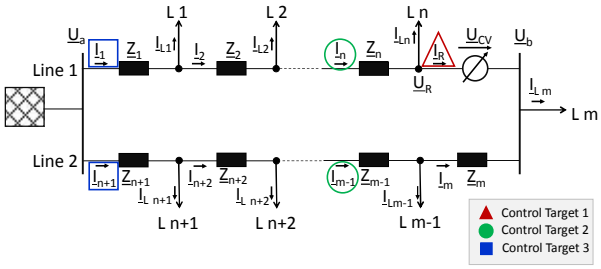

Fig. 1: Network with an indefinite number of loads

$$\underline{U}_{CV} = -\underline{I}_R \cdot \sum_{i=1}^{m} \underline{Z}_i - \sum_{i=1}^{n} \left(\underline{I}_{Li} \cdot \sum_{j=i}^{n} \underline{Z}_j \right) + \sum_{i=n+1}^{m} \left(\underline{I}_{Li} \cdot \sum_{j=n+i}^{m} \underline{Z}_j \right) = -\underline{I}_R \cdot \sum_{i=1}^{m} \underline{Z}_i + \underline{U}_{LC} \quad (1)$$

$$\underline{U}_{LC} = -\sum_{i=1}^{n} \left(\underline{Z}_i \cdot \sum_{j=i}^{n} \underline{I}_{Lj} \right) + \sum_{i=n+1}^{m} \left(\underline{Z}_i \cdot \sum_{j=n+i}^{m} \underline{I}_{Lj} \right) \quad (2)$$

For $\underline{U}_{CV} = 0$, which is the case for the controller standby mode, $\underline{U}_{LC}$ can be easily derived as:

$$\underline{U}_{CV} = 0 \Rightarrow \underline{U}_{LC,0} = \underline{I}_{R,0} \cdot \sum_{i=1}^{4} \underline{Z}_i \quad (3)$$

By measuring the current $\underline{I}_R$ and with the last set $\underline{U}_{CV}$, the voltage $\underline{U}_{LC}$ can be adjusted continually during operation:

$$\underline{U}_{LC} = \underline{U}_{CV} + \underline{I}_R \cdot \sum_{i=1}^{4} \underline{Z}_i \quad (4)$$

CONTROL TARGETS

In the following, the three most important control targets for controlling the current magnitudes are explained. The positions of the controlled currents are highlighted in Fig. 1. These values have to be measured by a sensor and transmitted to the PSR [5]. However, the voltage angles of the corresponding nodes in this locations cannot be measured. Hence, the phase shift between $\underline{U}_i$ and $\underline{I}_i$ is taken as an approximation for the current angles φ_I.
Depending on the desired accuracy, the control voltages can be calculated in several iteration steps. For the presented control targets, (5) shows the calculation of $\underline{U}_{CV}$ in an iterative way over time. The index t stands for discrete time steps. It is also possible to switch to a

different set point or even a different control target by the knowledge of the last control voltage. $\Delta\underline{U}_{CV}$ can be calculated with the below presented control targets.

$$\underline{U}_{CV}^{(t+1)} = \Delta\underline{U}_{CV}^{(t)} + \underline{U}_{CV}^{(t)} \quad (5)$$

Control Target 1: $\underline{I}_R = \underline{I}_{R,set}$

Control target 1 is used to set $\underline{I}_R$ in the line section of the controller (Fig. 1, red triangle) to a set point $\underline{I}_{R,set}$. To fulfill the control target, $\Delta\underline{U}_{CV}$ can be estimated with (6):

$$\Delta\underline{U}_{CV}^{(t)} = -\underline{I}_{R,set} \cdot \sum_{i=1}^{m} \underline{Z}_i + \underline{U}_{LC}^{(t)} = \left(\underline{I}_R^{(t)} - \underline{I}_{R,set}\right) \cdot \sum_{i=1}^{m} \underline{Z}_i \quad (6)$$

Control Target 2: $\underline{I}_x = \underline{I}_{x,set}$

The method for control target 1 can be used in a similar way for any current in a different line section (Fig. 1, green circle). It is assumed that the PSR drives an additional current $\Delta\underline{I}$ through the mesh which adds to all line currents $\underline{I}_i$ while the load currents remain unchanged. This is achieved by the control voltage and leads with (6) and (7) to (8):

$$\underline{I}_{x,set} = \underline{I}_x + \Delta\underline{I} \quad \Rightarrow \quad \underline{I}_{R,set} = \underline{I}_R - \Delta\underline{I} = \underline{I}_R - \left(\underline{I}_{x,set} - \underline{I}_x\right) \quad (7)$$

$$\Rightarrow \qquad \Delta\underline{U}_{CV}^{(t)} = \left(\underline{I}_{x,set} - \underline{I}_x^{(t)}\right) \cdot \sum_{i=1}^{m} \underline{Z}_i \quad (8)$$

Control Target 3: $\underline{I} = \underline{I}_1 = \underline{I}_{n+1}$

In order to guarantee a uniform utilization of both feeders, the currents I_1 and I_{n+1} should have equal magnitudes (Fig. 1, blue rectangles). In the uncontrolled case, the currents usually have different magnitudes which results in a current difference $\Delta\underline{I}$ (9).

$$\underline{I}_1 \neq \underline{I}_{n+1}: \quad (9)$$

$$\underline{I}_1 + \Delta\underline{I} = \underline{I}_{n+1} - \Delta\underline{I} \quad \Rightarrow \qquad \Delta\underline{I} = \frac{\underline{I}_{n+1} - \underline{I}_1}{2}$$

Following the same argument as for control target 2, current $\underline{I}_R$ has to be set with (6) and (9):

$$\underline{I}_{R,set} = \underline{I}_R - \Delta\underline{I} = \underline{I}_R - \frac{\underline{I}_{n+1} - \underline{I}_1}{2}$$
$$\Rightarrow \Delta\underline{U}_{CV}^{(t)} = \frac{\underline{I}_1^{(t)} - \underline{I}_{n+1}^{(t)}}{2} \cdot \sum_{i=1}^{m} \underline{Z}_i \quad (10)$$

Estimation of Mesh Impedance

The aforementioned sum of grid impedances $\Sigma\underline{Z}_i$, following denoted as $\underline{Z}_{mesh}$, can be estimated autonomously by the PSR. This advantage reduces the planning efforts and increases the flexible use of the regulator.

In a first step the regulator sets its voltage magnitude to a low tap $\underline{U}_{CV}^{(t)}$ and measures the current $\underline{I}_R^{(t)}$. Afterwards it reruns this procedure with a slightly increased $\underline{U}_{CV}^{(t+1)}$. By using (1), (2) and (11), (12) is easily found.

$$\Delta\underline{U}_{LC} = \underline{U}_{CV}^{(t+1)} - \underline{U}_{CV}^{(t)} = \left(-\underline{I}_R^{(t+1)} + \underline{I}_R^{(t)}\right) \sum_{i=1}^{m} \underline{Z}_i \quad (11)$$

$$\Rightarrow \underline{Z}_{mesh} = \sum_{i=1}^{m} \underline{Z}_i = \frac{\underline{U}_{CV}^{(t+1)} - \underline{U}_{CV}^{(t)}}{\underline{I}_R^{(t)} - \underline{I}_R^{(t+1)}} = \frac{\Delta\underline{U}_{CV}^{(t)}}{\underline{I}_R^{(t)} - \underline{I}_R^{(t+1)}} \quad (12)$$

Test Case for the Estimation of Mesh Impedance

For the validation of the estimation process for $\underline{Z}_{mesh}$ (12) a synthetic grid (Fig. 1) - with 20 loads, 10 PV in-feeds - and a real grid - with 113 loads, 38 PV in-feeds - were used. A simulation with load time series [6] for the period of one year results in Fig. 2 which shows the deviation of Z_{mesh} during a day. The most accurate value can be estimated in the time between 0 and 4 o'clock. Even though the deviation at midday with less than ±2% is also very low.

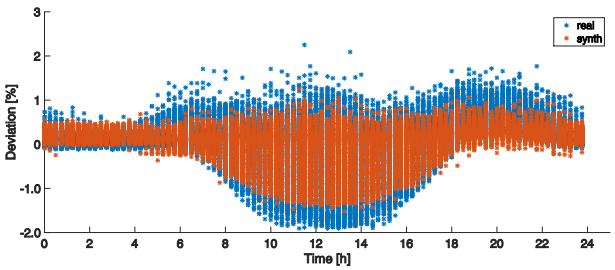

Fig. 2: Deviation of Z_{mesh} per hour for both test grids

In further studies the relation between the mesh impedance deviation and possible topology changes, due to e. g. blown fuses or conductor breaks, will be examined. Possibly, the PSR could monitor relevant impedance changes and notify the grid operator.

DESIGN OF THE PSR

Discrete Control Voltage Magnitude and Angle

In several tests with a synthetic and a real grid the effectiveness of an ideal PSR was tested. For different desired values the control targets meet the required set points with small deviations [4].

The ideal regulator could set the angle of the control voltage to its calculated exact value. For a realistic PSR, continuous angles could only be generated by the use of complex power electronics. For costs reason and service life a simple implementation is sought which can be realized by easy-to-build transformer circuit technology. Therefore, the possible adjustable voltage angles have been reduced to a selection of discrete values which were chosen based on their occurrence in former simulations:

$$\delta \in \{0°, 30°, 120°, 150°, 180°, 210°, 240°, 270°\}$$

Comparable to the control voltage angles, an easy to realize implementation of the control voltage magnitudes is to reduce them to discrete steps. Several studies showed, that the PSR can achieve the control targets with sufficient accuracy by a ΔU_{CV} rounded to 0.25%-steps.

Control Voltage Magnitude Circuit

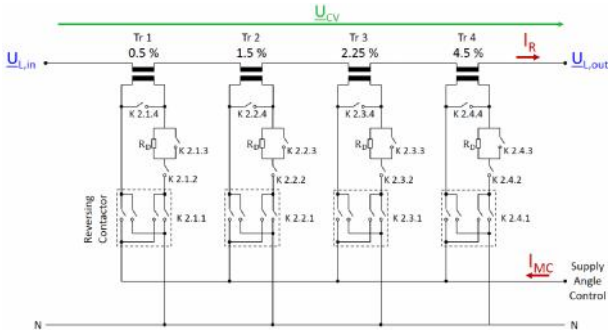

Fig. 3: MC circuit of a single phase

Fig. 3 shows the circuit for the CV magnitude control (MC) of a single phase. It basically consists of the transformers Tr 1 to Tr 4 in series connection. These can be switched independently. With the corresponding reversing contactors (RC) they can add or subtract their specified additional voltage to the line voltage. Table 1 shows the transformation ratios. Further relays and resistors R_D are used for switching operations and protection issues. The three MC circuits are supplied by the higher-level circuit for angle control (AC).

Table 1: Transformation ratio

MC transformer	Tr 1	Tr 2	Tr 3	Tr 4
Transformation ratio t_{Tr}	$t_1 = 1/200$	$t_2 \approx 1/67$	$t_3 \approx 1/44$	$t_4 \approx 1/22$
Applied voltage	0.5% $U_{L,out}$	1.5% $U_{L,out}$	2.25%	4.5% $U_{L,out}$

In case of the following considered three-phase systems, the aforementioned equations are extended with an indices $L \in \{1, 2, 3\}$ which stands for the conductors L1, L2, L3. The CV $\underline{U}_{CV}$ is defined as the voltage between the PSR connection points $\underline{U}_{L,in}$ and $\underline{U}_{L,out}$ (Fig. 3) and can be adjusted by the given transformation ratio t_{CV}:

$$\underline{U}_{CV,L} = \underline{U}_{L,in} - \underline{U}_{L,out} = t_{CV} \cdot \underline{U}_{L,out} \qquad (13)$$

The general calculation of the transformation ratios for each conductor $t_{CV,L}$ is represented by (14). Depending on the RC state, a transformer is either turned off (RC = 0), or applies its voltage with positive (RC = 1) or negative (RC = -1) sign to the conductor voltage.

$$t_{CV} = \sum_{Tr=1}^{4} RC_{Tr} \cdot (t_{Tr}) \quad \text{with} \quad RC_{Tr} = \begin{cases} +1 & \text{on} \\ 0 & \text{off} \\ -1 & \text{on (reversed)} \end{cases} \qquad (14)$$

From (14) follows that the CV magnitude can be impressed in the following steps by combining:

$$U_{CV} = \begin{cases} 0 \ldots \pm 6.75\% & \text{in } \pm 0.25\% \\ \pm 6.75\% \ldots \pm 8.75 & \text{in } \pm 0.50\% \end{cases} \text{ of } U_{L,out}$$

U_{CV} is given in percent of the conductor voltage $U_{L,out}$.

Control Voltage Angle Circuit

The angles of the CV can be controlled by the circuit in Fig. 4 which generates the supply voltage for the MC circuits. The angle of the supply voltage appends to the CV magnitudes. The phase shifter (PS) in 'Dyn11' vector group generates a secondary voltage with a 30° phase shift. With the relay matrix in the center of Fig. 4 the supply voltage for the MCs can be selected individually according to the required angle.

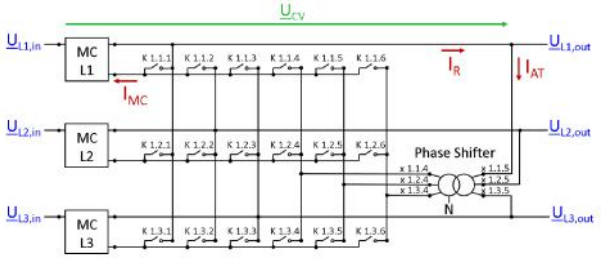

Fig. 4: Circuit for angle control

Depending on the switch state of the relays and the RCs, the CV angle can be set in 30° steps. Table 2 shows the possible angles and the corresponding switched relays. The relay designation depends on the driven MC circuits which is therefore replaced by '~'. The CV angle is relative to the phase controlled by the MC circuits. The aforementioned selection of angles is marked red.

Table 2: Switchable Angles by Relay Matrix

			CV Angle aδ											
	Relay	$a\varphi_U$	0	30	60	90	120	150	180	210	240	270	300	330
Grid	K1.~.1	0	X											
	K1.~.3	120					X						X	
	K1.~.2	240			X						X			
PS	K1.~.4	30		X						X				
	K1.~.6	150						X						X
	K1.~.5	270				X						X		
RC	K2.*.~	180			X	X			X	X			X	X

~ : MC L1...MC L3 * : Tr 1...Tr 4

Asymmetric load

As already mentioned, the AC circuit supplies the MC circuits. Due to the effect of asymmetric loadings and individually set CVs, the conductor voltages can differ. Caused by the relay matrix method, this can have an influence on the calculation of the transformation ratio t_{CV} which has to be set for the required $\underline{U}_{CV,L}$.

In Fig. 4 is seen that e. g. MC_{L1} is supplied by conductor L2, if an angle of 240° is necessary. Thus, the magnitude of $\underline{U}_{L2,out}$ has an influence on the supply voltage of MC_{L1}, which results in a correct angle but a possibly different voltage magnitude.

As consequence, $t_{CV,1}$ has to be adjusted, what can be solved with (15). By calculating a correction value consisting of $U_{1,out}$ and $U_{2,out}$, a corrected transformation ratio can be determined. Because of the 0.25% steps, a rounded $\tilde{t}_{CV}$ is the results. This estimation must be executed individually for each conductor.

$$\underline{U}_{CV,1}^{(t)} = t_{CV,1} \cdot U_{2,out}^{(t)} \cdot e^{j\varphi_{U_2}} \cdot \frac{U_{1,out}^{(t)}}{U_{2,out}^{(t)}} \approx \tilde{t}_{CV,1} \cdot \underline{U}_{CV,2}^{(t)}$$
$$\text{with} \quad \tilde{t}_{CV,1} = \text{round}_{0.25}\left(t_{CV,1} \cdot \frac{U_{CV,1}^{(t)}}{U_{CV,2}^{(t)}} \right) \qquad (15)$$

Dimensioning of Components

The circuits for magnitude and angle control were implemented in the simulation environment LTspice®. For the dimensioning of the components, the shown control targets were tested and the resulting currents measured. For a typical grid operation, the PSR must be able to carry currents up to 200 A, if it is used to protect against excessive currents. This leads to a simulation with a 150 kVA regulator for a symmetric load case. Four CV magnitudes with all feasible angles were simulated. The measured currents are shown in Fig. 4. Table 3 represents the highest occurring currents. The values are used for the dimensioning of the components for the prototype.

Table 3: Current Values for a 150 kVA Regulator

U_{CV}	I_R [A]	I_{PS} [A]	I_{MC} [A]
0%	215.8	2.3	0
1% ∠210°	219.4	4.8	2.7
4.5% ∠210°	232.1	12.7	10.7
8.75% ∠210°	253.6	25.3	23.2

SIMULATION OF THE PSR DESIGN

Symmetric Load Simulation

In a simulation with the explained circuits, the desired CV values $U_{CV,set}$ were compared to the simulated actual values $U_{CV,sim}$ for a selection of regulator taps (Table 4). It can be seen that the $U_{CV,sim}$ magnitudes differ slightly from the desired values. This is caused by the taped voltages for the MC circuit supply, which are influenced by the set regulator tap. However, compared to the 30° steps, the variations are so slight, that they can be neglected.

Table 4: CV desired and actual values

Tap [%]	0	0.5	1.5	2.25	4.5	8.75	8.75 Δ30°	8.75 Δ120°	8.75 Δ180°	8.75 Δ240°
$\underline{U}_{CV,set}$ [V]	0	1.150	3.450	5.175	10.350	20.125	20.125 ∠30°	20.125 ∠120°	20.125 ∠180°	20.125 ∠240°
$\underline{U}_{CV,sim}$ [V]	0.012	1.148	3.382	5.035	9.829	18.434	18.733 ∠27.7°	20.841 ∠115.4°	20.876 ∠180°	20.873 ∠244.5°

Asymmetric Load Simulation

In a further simulation the PSR was loaded highly asymmetrically resulting in varying conductor voltages (Table 5, line 1). U_{CV} was assumed with 4.5% and an angle of 120°. To establish the required phase shift, the tapped conductors are given in line 2. The calculated exact value of $\underline{U}_{CV,L}$ is shown in the following line. In a first step the simulation was made with the unadjusted t_{CV} and results in the voltages of line 5. After calculating an adjusted $\tilde{t}_{CV}$ with (15) (line 6) the subsequent simulation results in the values of line 7. The deviations are given in lines 8 and 9, which show, that $\tilde{t}_{CV}$ improved the deviation of the required $\underline{U}_{CV}$.

Table 5: Asymmetric Load Case

		L1		L2		L3	
1	$U_{L,out}$ [V]	238.52		221.51		236.14	
2	Tap	L3		L1		L2	
3	calculated $\underline{U}_{CV,L}$[V]	10.39 V $e^{j120°}$		10.39 V $e^{j120°}$		10.39 V $e^{j120°}$	
4	with t_{CV}	4.5%		4.5%		4.5%	
5	$U_{CV,L}(t_{CV})$ [V]	10.45 V $e^{j119.6°}$		11.08 V $e^{j120.1°}$		9.44 V $e^{j117.9°}$	
6	adjusted $\tilde{t}_{CV}$	4.5%		4.25%		4.75%	
7	$U_{CV,L}(\tilde{t}_{CV})$ [V]	10.45 V $e^{j119.5°}$		10.49 V $e^{j120.2°}$		9.98 V $e^{j118.1°}$	
8	$\Delta U(t_{CV})$ [V]	$\Delta\delta$ [°]	-0.06V	0.5°	-0.69V	-0.1°	0.95V	2.1°
9	$\Delta U(\tilde{t}_{CV})$ [V]	$\Delta\delta$ [°]	-0.06V	0.5°	-0.1V	-0.2°	0.41V	1.9°

CONCLUSION

Assuming that more PV systems shall be integrated into the LV-networks in the future, gaining control of power flow in meshed LV-networks gets increasingly important. By impressing a control voltage at a suitable phase angle by means of a special PSR the power flow can be controlled to a certain limit in order to prevent thermal overloads. This will allow a further integration of renewable generators to the grid without classical network extensions. This paper shows a scheme to determine the control voltage allowing the PSR to control the current flow in different line sections. The presented design provides the basics for a PSR prototype. Further work will concentrate on the implementation of the control scheme and to run tests in the lab and subsequently in network operation of a real LV-grid.

REFERENCES

[1] S. Bhattacharyya, P. Karremans, 2015, “Estimating the impact of Large Scale Photovoltaic Generations on an meshed Low Voltage Network – A Case Study Results” CIRED Conference, Lyon, France

[2] J. Schlabbach, 1995, *Elektroenergieversorgung – Betriebsmittel und Auswirkungen der elektrischen Energieverteilung*, VDE-Verlag GmbH, Berlin, Germany

[3] D. De Santis, G. Abbatantuono, et. al., „Feasibility of power flow control on LV distribution systems“, *Advances in Engineering Mechanics and Materials*, no. 33, 2014

[4] S. Lang, W. H. Wellssow, 2016, “Power Flow Control with Phase Shifting Regulators in meshed Distribution Grids”, to be published: IEEE PES General Meeting, Boston, USA

[5] “Kommunikationstechnik für intelligente Stromnetze mittels Breitband-Powerline“, *netzpraxis*, no. 48, 2009

[6] H. Rui, W. H. Wellssow and P. Hauffe, 2014, “Applying the Smart Grid Metric Framework to Asses Demand Side Integration in LV Grid Congestion Management”, CIRED Workshop, Rome, Italy